Next-nearest neighbour forces in diatomic superlattices

1991 J. Phys.: Condens. Matter 3 9697

(http://iopscience.iop.org/0953-8984/3/48/011)

J. Phys.: Condens. Matter 3 (1991) 9697–9703. Printed in the UK

Next-nearest neighbour forces in diatomic superlattices

R Hadizad, D R Tilley and J Tilley
Department of Physics, University of Essex, Wivenhoe Park, Colchester CO4 3SQ, UK

Received 15 August 1991

Abstract. Results are presented for phonons in a 1D diatomic model superlattice. Each frequency ω corresponds to two Bloch wavenumbers Q_1 and Q_2. For $\alpha < 0.25$, where α is the ratio of next-nearest to nearest force constants, the results are essentially a perturbation of those found with nearest-neighbour forces only. For $\alpha > 0.25$, however, qualitatively new results are found, and in particular both Q_1 and Q_2 can be real over some frequency range. Illustrative dispersion curves are presented.

1. Introduction

In a previous paper (Hadizad *et al* 1991, referred to as I) we gave a detailed discussion of the effect of including next-nearest neighbour (NNN) forces in the lattice dynamics of a 1D monoatomic superlattice. The general background and motivation were covered in I. Although NNN forces have been included in other lattice-dynamical calculations, it appears that some of the qualitative results for the bulk lattice derived in I are new. In particular, when the ratio $\alpha = C_2/C_1$ of NNN to nearest-neighbour (NN) force constants exceeds the value 0.25, there is a frequency interval in which two real values q_1 and q_2 of wavevector are found in the bulk material. In consequence, for $\alpha > 0.25$ the folded acoustic-mode spectrum of a superlattice takes a more elaborate form than in the NN model.

In this paper, we extend the results of I to a 1D diatomic superlattice. The most important difference between the bulk diatomic and monatomic lattices is the appearance in the former case of the optic-phonon branch in addition to the acoustic-phonon branch. In a diatomic superlattice, both optic and acoustic phonon branches are folded into the mini Brillouin zone $-\pi/L < Q < \pi/L$, where L is the superlattice period. The nature of the optic phonons depends upon the frequency intervals occupied by the optic-phonon bands of the two components of the superlattice (see Sapriel and Djafari-Rouhani 1989). If there is no overlap between these intervals, as in GaAs/AlAs for example, then the lattice displacements in an optic mode of the superlattice are largely restricted to the component in which a bulk optic phonon propagates, and the dispersion curve of the mode is very flat (ω almost independent of Q). It is then customary to speak of *confined* optic phonons. On the other hand, if the optic-phonon bands overlap, as in the GaAs reststrahl region of GaAs/$Al_xGa_{1-x}As$ for example, there is more dispersion in the superlattice optic modes (Albuquerque *et al* 1988).

In section 2 we review the lattice dynamics of a bulk diatomic 1D crystal including NNN forces. Like the monatomic crystal, the addition of NNN forces means that four

0953-8984/91/489697 + 07 $03.50

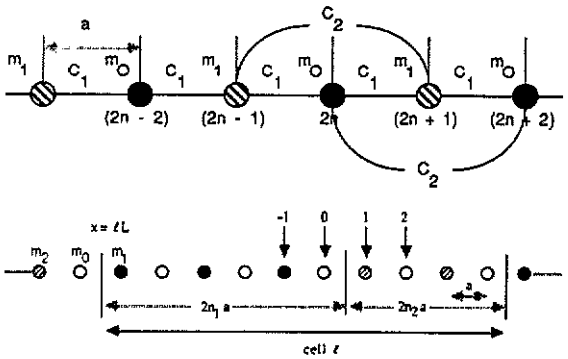

Figure 1. (*a*) Bulk 1D diatomic NNN crystal, with notation defined. (*b*) Superlattice model for section 3. Spring constants are the same throughout as in (*a*).

values of wavenumber q, namely $\pm q_1$, $\pm q_2$, are allowed for each frequency, rather than the two that occur with NN forces only. In general, of course, q_1 and q_2 are not both real.

Next, we discuss a superlattice model in which the atomic masses in component 1 are m_0 and m_1, those in component 2 are m_0 and m_2 while the force constants are the same throughout. This may be seen as a simple model corresponding to $GaAs/Al_xGa_{1-x}As$, and it is sufficiently general to bring out qualitative points of interest. The formal results, presented in section 3, are very similar to those for the monatomic superlattice. Since there are four values of q, the transfer matrix $\mathbf{T}$ is 4×4. $\mathbf{T}$ is easily shown to be unimodular, $\det \mathbf{T} = 1$, so that the eigenvalues satisfy $\lambda_1\lambda_2\lambda_3\lambda_4 = 1$ and in fact occur as two pairs $(\lambda_1, \lambda_1^{-1})$ and $(\lambda_2, \lambda_2^{-1})$. Bloch vectors Q_n are defined by $\exp(iQ_nL) = \lambda_n$. The formal results are illustrated in section 3 with graphs of dispersion curves, and a brief discussion is given in section 4.

2. Bulk crystal

We consider the model shown in figure 1(*a*), in which masses m_0 at positions $2na$ alternate with masses m_1 at positions $(2n + 1)a$. NN and NNN force constants C_1 and C_2 are defined as shown. The equations of motion for the two species of atom are

$$-m_0\omega^2 u_{2n} = C_1(u_{2n-1} + u_{2n+1} - 2u_{2n}) + C_2(u_{2n-2} + u_{2n+2} - 2u_{2n}) \tag{1}$$

$$-m_1\omega^2 u_{2n+1} = C_1(u_{2n} + u_{2n+2} - 2u_{2n+1}) + C_2(u_{2n-1} + u_{2n+3} - 2u_{2n+1}). \tag{2}$$

These are solved with the *ansatz*

$$u_{2n} = u_0 \exp(2inqa) \tag{3}$$

$$u_{2n+1} = u_1 \exp[i(2n + 1)qa]. \tag{4}$$

Equations (1) and (2) lead to two expressions for $r = u_1/u_0$:

$$r = 2C_1 \cos qa/(-m_1\omega^2 + 4C_2 \sin^2 qa + 2C_1)$$

$$= (-m_0\omega^2 + 4C_2 \sin^2 qa + 2C_1)/2C_1 \cos qa. \tag{5}$$

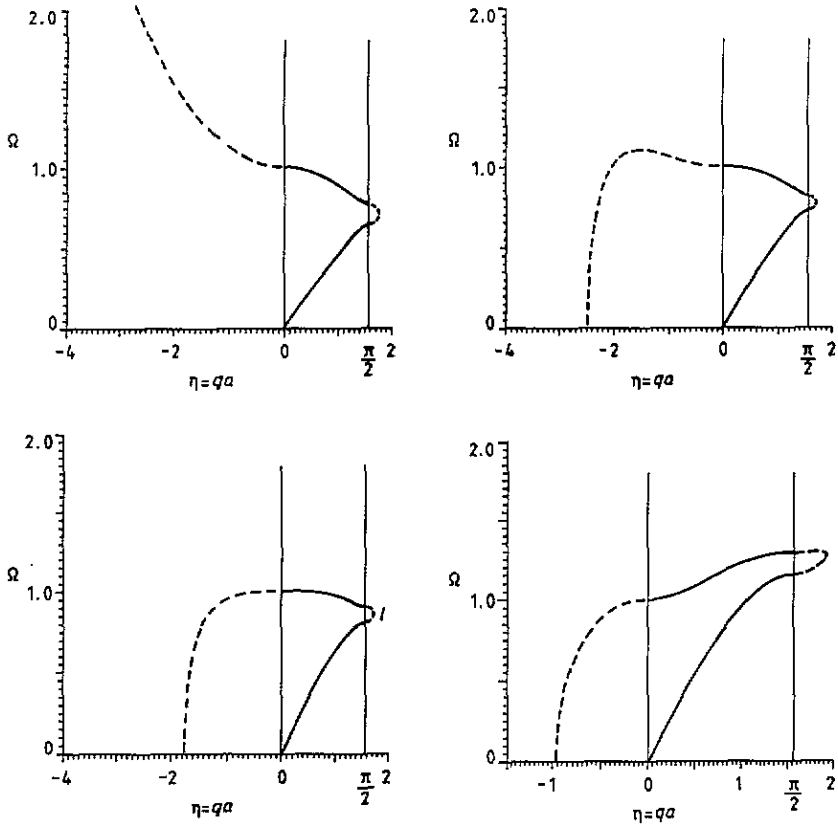

Figure 2. Bulk dispersion curves, Ω versus $\eta = qa$. Complex η of the form $\pi/2 + iy$ is represented as a broken curve with y as the abscissa measured from $\eta = \pi/2$, while iy is represented as a broken curve with y as the negative of the abscissa measured from $\eta = 0$. (*a*) NN crystal ($\alpha = 0$) for $\gamma = m_0/m_1 = 0.7$. (*b*) $\alpha = 0.1$ and $\gamma = 0.8$. (*c*) $\alpha = 0.25$ and $\gamma = 0.8$. (*d*) $\alpha = 1.0$ and $\gamma = 0.8$.

This gives the dispersion equation, which is conveniently written as a quadratic equation for $\sin^2 qa$:

$$16C_2^2 \sin^4 qa + [16C_1C_2 - 4C_2\omega^2(m_0 + m_1) + 4C_1^2] \times \sin^2 qa + [m_0m_1\omega^4 - 2C_1\omega^2(m_0 + m_1)] = 0. \tag{6}$$

For a given ω, this has solutions $\sin qa = \pm A^{1/2}, \pm B^{1/2}$, so that the wavevectors do indeed occur in pairs $\pm q_1, \pm q_2$, which of course need not be real.

Equation (6) is in a convenient form for numerical solution, and various cases are illustrated in figure 2. The frequency is scaled as $\Omega = \omega/\omega_0$, where

$$\omega_0^2 = 2C_1(1/m_0 + 1/m_1) \tag{7}$$

which will be recognised as the frequency at the top of the optic-phonon band ($q = 0$

point) for the NN crystal. Two parameters are involved in (6), namely the ratio of the force constants

$$\alpha = C_2/C_1 \tag{8}$$

and the ratio of the masses

$$\gamma = m_1/m_0. \tag{9}$$

Figure 2(*a*) shows the well known NN dispersion curve for $\gamma = 0.7$. With the notation of figure 1(*a*), the Brillouin-zone edge is at $\eta = qa = \pi/2$. Figure 2(*a*) recalls that for $\gamma \neq 1$ there is a stop band between the acoustic and optic branches in which η performs an excursion off the real axis, $\eta = \pi/2 + iy$. In fact a surface mode on the semi-infinite diatomic lattice is found within this stop band (Wallis 1957, Cottam and Tilley 1989). We also show in figure 2(*a*) the imaginary solution $\eta = iy$ found for $\Omega > 1$.

A key feature of the monatomic case is that $\alpha = 0.25$ is a critical value of this ratio. Although there are two values of q for each frequency, only one is real for $\alpha < 0.25$. However, for $\alpha > 0.25$ there is a frequency interval in which both values of q are real. Exactly the same is true for the diatomic crystal, as illustrated in figures 2(*b*) to 2(*d*). In figure 2(*b*) it is seen that for small α the second root appears, but takes the form iy with y fairly large, so it is not of great physical significance. Figure 2(*c*) is for the critical value $\alpha = 0.25$, and shows a very flat dispersion curve (the first three derivatives $d^n\omega/dq^n$ vanishing) at the top of the optic-phonon band. Figure 2(*d*), for the large value $\gamma = 1.0$, shows how the point $q = 0$, $\Omega = 1$ on the optic-phonon band becomes a minimum for $\alpha > 0.25$, with the lower part of the optic band and the upper part of the acoustic band overlapping to give two real values of q in some frequency range above $\Omega = 1$. Comparison of figures 2(*b*) to 2(*d*) also shows how the root $\eta = iy$ moves closer to the origin as α increases.

One way of understanding the NN diatomic dispersion curve, figure 2(*a*), is to start from the monatomic crystal with $m_0 = m_1$, in which case a simple acoustic-phonon dispersion curve is found in the Brillouin zone $0 \leqslant \eta \leqslant \pi$. If m_1 is now taken slightly different from m_0, the dispersion curve folds into the reduced zone $0 \leqslant \eta \leqslant \pi/2$ appropriate to the diatomic crystal. As the ratio m_1/m_0 varies further from zero a gap opens at the zone edge $\eta = \pi/2$, resulting in a curve like that shown in figure 2(*a*). In a similar way, the dispersion curves of figures 2(*b*) to 2(*d*) may be seen as resulting from folding of the corresponding monatomic NNN dispersion curves, shown as figures 2(*a*) and 2(*b*) of I.

3. Superlattice

We consider the superlattice model shown in figure 1(*b*). A unit cell of the superlattice consists of $n_1(m_0, m_1)$ pairs followed by $n_2(m_0, m_2)$ pairs, so that the unit cell has length $L = 2(n_1 + n_2)a$. Since the spring constants are taken to be the same throughout, the only difference between the two components of the superlattice is in the occurrence of the two different masses m_1 and m_2.

The derivation of the dispersion equation follows along very similar lines to that for the monatomic superlattice. The displacements at frequency ω for an atom at position x in unit cell l, component 1 can be written

$$u_{0l} = a_l^{\mathrm{L}} \exp[\mathrm{i}q_{11}(x - lL)] + b_l^{\mathrm{L}} \exp[-\mathrm{i}q_{11}(x - lL)] + c_l^{\mathrm{L}} \exp[\mathrm{i}q_{12}(x - lL)] + d_l^{\mathrm{L}} \exp[-\mathrm{i}q_{12}(x - lL)] \tag{10}$$

for an atom of mass m_0, and

$$u_{1l} = a_l^{\mathrm{L}} r_{11} \exp[\mathrm{i}q_{11}(x - lL + a)] + b_l^{\mathrm{L}} r_{11} \exp[-\mathrm{i}q_{11}(x - lL + a)] + c_l^{\mathrm{L}} r_{12} \exp[\mathrm{i}q_{12}(x - lL + a)] + d_l^{\mathrm{L}} r_{12} \exp[-\mathrm{i}q_{12}(x - lL + a)] \tag{11}$$

for an atom of mass m_1. Here q_{11} and q_{12} are the two solutions of the bulk dispersion equation (6) for the given frequency, while r_{11} and r_{12} are given by (5) with variables q_{11} or q_{12}. The superscripts L indicate that the phases in the exponential factors are referred to the left-hand end of the cell at $x = lL$. As for the monatomic case, amplitudes a_l^{R} etc. can be introduced by similar definitions to (10) and (11) but with $x - lL - 2n_1 a$ replacing $x - lL$. The vectors $|U^{\mathrm{L}}\rangle = (a_l^{\mathrm{L}} b_l^{\mathrm{L}} c_l^{\mathrm{L}} d_l^{\mathrm{L}})^{\mathrm{T}}$ and $|U^{\mathrm{R}}\rangle = (a_l^{\mathrm{R}} b_l^{\mathrm{R}} c_l^{\mathrm{R}} d_l^{\mathrm{R}})^{\mathrm{T}}$ are related by

$$|U^{\mathrm{R}}\rangle = \mathbf{F}_1 |U^{\mathrm{L}}\rangle \tag{12}$$

where $\mathbf{F}_1$ is the diagonal matrix $[f_{11}\bar{f}_{11}f_{12}\bar{f}_{12}]$ with

$$f_{1j} = \exp(2\mathrm{i}q_{1j}n_1 a) \qquad \bar{f}_{1j} = f_{1j}^{-1} \qquad j = 1, 2. \tag{13}$$

The displacements in component 2 are described similarly by vectors $|W^{\mathrm{L}}\rangle$ and $|W^{\mathrm{R}}\rangle$ related by a phase matrix $\mathbf{F}_2$.

The vectors $|W_l^{\mathrm{L}}\rangle$ and $|U_l^{\mathrm{R}}\rangle$ are related by the equations of motion of the four atoms at the interface, marked in figure 1(*b*):

$$\mathbf{M}_1 |U_l^{\mathrm{R}}\rangle = \mathbf{M}_2 |W_l^{\mathrm{L}}\rangle \tag{14}$$

where

$$\mathbf{M}_j = \begin{pmatrix} 1 & 1 & 1 & 1 \\ r_{i1}\bar{s}_{i1} & r_{i1}s_{i1} & r_{i2}\bar{s}_{i2} & r_{i2}s_{i2} \\ s_{i1}^2 & \bar{s}_{i1}^2 & s_{i2}^2 & \bar{s}_{i2}^2 \\ r_{i1}s_{i1} & r_{i1}\bar{s}_{i1} & r_{i2}s_{i2} & r_{i2}\bar{s}_{i2} \end{pmatrix} \tag{15}$$

and

$$s_{ij} = \exp(\mathrm{i}q_{ij}a) \qquad \bar{s}_{ij} = s_{ij}^{-1}. \tag{16}$$

Finally the transfer matrix $\mathbf{T}$ is defined by

$$|U_{l+1}^{\mathrm{L}}\rangle = \mathbf{T}|U_l^{\mathrm{L}}\rangle = \mathbf{M}_1^{-1}\mathbf{M}_2\mathbf{F}_2\mathbf{M}_2^{-1}\mathbf{M}_1\mathbf{F}_1 |U_l^{\mathrm{L}}\rangle \tag{17}$$

which is formally identical to the expression for the monatomic superlattice.

As for the monatomic case, we have used a symbolic algebra package (Macsyma) to find analytic expressions for the elements of $\mathbf{T}$ and the results are given elsewhere (Hadizad 1991). Here we proceed straight to numerical illustrations of dispersion curves

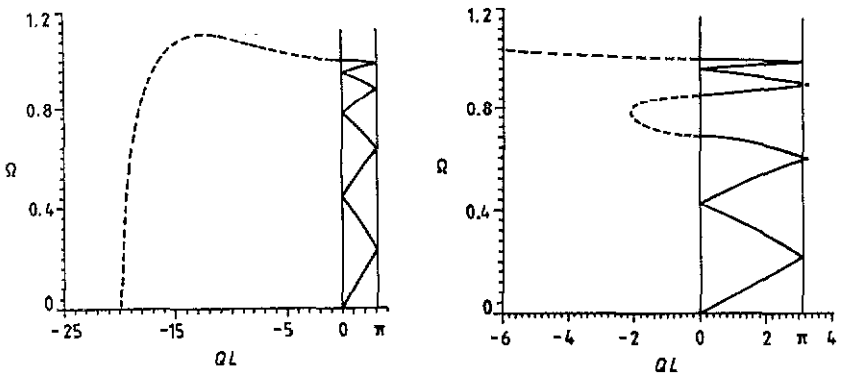

Figure 3. Superlattice dispersion curves, Ω versus QL, where Ω is defined as previously. The curves are for a 4 + 4 superlattice with force-constant ratio $\alpha = 0.1$. (*a*) $\gamma_1 = m_1/m_0 = 1.0$ and $\gamma_2 = m_2/m_0 = 1.0$. (*b*) $\gamma_1 = 0.7$ and $\gamma_2 = 0.6$.

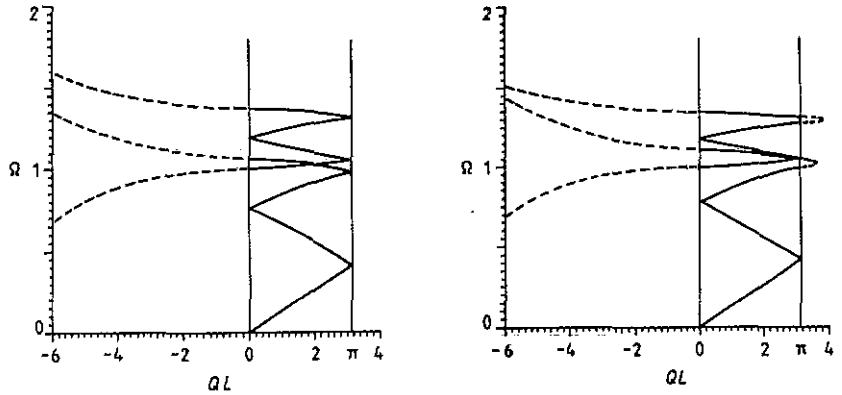

Figure 4. Superlattice dispersion curves for a 4 + 4 superlattice with $\alpha = 1.0$. (*a*) $\gamma_1 = \gamma_2 = 0.6$. (*b*) $\gamma_1 = 0.7$ and $\gamma_2 = 0.6$.

ω versus QL, where the Bloch wavevectors Q are related to the eigenvalues λ of $\mathbf{T}$ by the relation stated in section 1:

$$\exp(\mathrm{i}QL) = \lambda. \tag{18}$$

Figure 3 is concerned with a small value of the force-constant ratio α. In figure 3(*a*) we show the dispersion curves for a 4 + 4 superlattice with all masses equal, $\gamma_1 = \gamma_2 = 1$. This is very close to a simple folding into the mini Brillouin zone of a dispersion curve like figure 2(*a*) or 2(*b*), or indeed since the masses are equal within each component it is simply the folding of a bulk *monatomic* dispersion curve. As we have emphasized throughout, there are two Bloch vectors Q for each frequency, but one of the roots is imaginary everywhere and of rather large magnitude, so it is not of great physical significance. For large enough frequency, $\Omega \geqslant 1.1$, both roots for Q are complex and are not represented on the figure. Figure 3(*b*) differs from figure 3(*a*) in having mass ratios different from unity and different from each other. In order to bring out the

structure in the mini Brillouin zone, most of the second (pure imaginary) Bloch vector has been omitted. In this case, because γ_1 and γ_2 are both quite different from unity, the distinction between acoustic and optic branches is maintained in the superlattice. Since α is small, the figure is very close to the picture of folded acoustic modes together with confined optic modes that is found with NN forces and which is the paradigm for interpretation of Raman scattering experiments.

For large α we are concerned with folding into the mini Brillouin zone bulk dispersion curves like that in figure 2(*d*). Here the frequency ranges of the acoustic and optic branches overlap. Figure 4(*a*) shows the dispersion curves for a 4 + 4 superlattice in which the two components are in fact identical: the relationship with figure 2(*d*) and the overlap of the acoustic and optic branches is quite clear. Figure 4(*b*) shows the evolution of figure 4(*a*) when the two components differ; stop bands appear, and the overlap between the branches becomes more complicated.

4. Discussion

We have derived and illustrated the dispersion equations for a 1D diatomic superlattice with both NN and NNN forces. This is a significant extension of our previous work on monatomic superlattices since, firstly, there is now an optic as well as an acoustic branch and secondly, many of the experimental systems are diatomic. The general structure of the problem is similar to that found for the monatomic superlattice, in that one is dealing with two pairs of bulk wavevectors $\pm q_1$ and $\pm q_2$ and for the superlattice with two pairs of Bloch vectors $\pm Q_1$ and $\pm Q_2$. As in the monatomic case, although the dispersion curves can look quite complicated, they can usually be interpereted in terms of simple ideas about folding into the mini Brillouin zone. The value 0.25 of the force-constant ratio $\alpha = C_2/C_1$ is once again critical. For $\alpha < 0.25$, the NNN forces produce no more than a perturbation on the results found with NN forces, but for $\alpha > 0.25$ some qualitatively new results appear.

References

Albuquerque E L, Fulco P and Tilley D R 1988 *Phys. Status Solidi* b **146** 449
Cottam M G and Tilley D R 1989 *Introduction to Surface and Superlattice Excitations* (Cambridge: Cambridge University Press)
Hadizad R 1991 *PhD Thesis* University of Essex
Hadizad R, Tilley D R and Tilley J 1991 *J. Phys.: Condens. Matter* **3** 291
Sapriel J and Djafari-Rouhani B 1989 *Surf. Sci. Rep.* **10** 189
Wallis R F 1957 *Phys. Rev.* **116** 302